Tech Science Press

Improving the Antibacterial Property of Chitosan Hydrogel Wound Dressing with Licorice Polysaccharide

Haiwei Ren[1], Li Wang[1], Hui Bao[1], Yunya Xia[1], Dada Xu[1], Weijie Zhang[1,*] and Zhiye Wang[2]

[1]School of Life Science and Engineering, Lanzhou University of Technology, Lanzhou, 730050, China
[2]Institute of Biology, Gansu Academy of Sciences, Lanzhou, 73000, China
*Corresponding Author: Weijie Zhang. Email: twz1514@126.com

Abstract: A series of hydrogels with different ratios of chitosan and licorice polysaccharide (LP) were prepared by crosslinking to different concentrations of genipin (gp). They were characterized by FTIR (Fourier transform infrared spectroscopy), SEM (Scanning electron microscope), swelling ratio, rheological measurements, degradation with time, cytotoxicity, and antibacterial efficacy. Results show that the hydrogels have porous structures. With an increase in LP content, the swelling rate grows in the early stage of immersion in buffer and drops later. The swelling ratio ranged from 986% to 1677%, and stiffness varied from 777 Pa to 1792 Pa. The addition of LP reduced the mechanical strength and delayed gelation and degradation of the hydrogels. However, the most important discovery was that gp increases the viability of NIH 3T3 cells from 94% to 137%, and LP raises the bacteriostatic efficacy from 51% to 78%. Hydrogels synthesized from 1% genipin, 3% chitosan, and 4% licorice polysaccharide showed the best antibacterial and fibroblast proliferation promoting activities. They exhibited moderate swelling and degradation rates over time, while being more suitable to affect healing of chronic wound infections. These results provide a new strategy to improve the antibacterial effectiveness and cyto-compatibility of chitosan hydrogels with water soluble active LPs from Glycyrrhiza that derive from traditional Chinese medicine.

Keywords: Chitosan; licorice polysaccharide; hydrogel; antibacterial property; wound dressing

1 Introduction

Wound dressing is an important pharmaceutical product for wound care. Traditional wound dressings, such as gauze and cotton wool, have the following disadvantages: the ability to remove exudates is limited, especially after being soaked by plasma. In addition, antiseptic protection is diminished behind a loose and fragile barrier, which raises the chance of exogenous infections [1]. One solution is to replace the traditional dressing with newly developed hydrogel dressings of various compositions. Hydrogel-based wound dressings are a promising material for wound healing [2]. Compared with traditional materials, hydrogel dressings can relieve pain, maintain a moist wound environment [3,4], inhibit or kill bacteria, and accelerate wound

healing. Furthermore, drug-loaded hydrogels have provided new options for the treatment of refractory wounds such as diabetic foot ulcers and other chronic ulcers, and which have produced impressive healing in animal wound models and show impressive clinical potential [5–8].

Chitosan (CS) is a low-cost, biocompatible and biodegradable natural polymer with activity that promotes cell proliferation. One important property is its bacteriostatic capacity. As a cationic macromolecular polysaccharide, CS can inhibit the growth of microbes through multiple mechanisms, such as disrupting the cell wall, interfering with protein synthesis, and chelating nutrients and essential metals, which makes it difficult for microbes to develop resistance [9]. Altogether, this makes CS an excellent substitute for antibiotics. Such properties make CS a very promising material for the development of hydrogel wound dressings. Much progress has been made to formulate CS into more compatible polymers for wound dressings and other applications (e.g., drug delivery, food packaging). These include composite materials prepared with the following co-factors:

a) Lignin nanoparticles and polyvinyl alcohol [10,11],
b) Antibacterial, anti-oxidant electroactive, and injectable hydrogels based on quaternized chitosan-g-polyaniline (QCSP) and benzaldehyde group functionalized poly(ethylene glycol)-co-poly(glycerol sebacate) (PEGS-FA) [12],
c) Conductive cryogels based on carbon nanotubes (CNT) and glycidyl methacrylate functionalized quaternized chitosan [13],
d) Antibacterial, adhesive, antioxidant, and conductive GT-DA/chitosan/CNT composite hydrogels based on gelatin-grafted-dopamine (GT-DA) and polydopamine-coated carbon nanotubes (CNT-PDA) [14], and
e) Self-healing nanocomposite hydrogels based on N-carboxyethyl chitosan (CEC) and benzaldehyde-terminated Pluronic F127/carbon nanotubes (PF127/CNT) [15].

A common deficiency of CS is its poor water solubility; this is the major limiting factor to its application as a bacteriostat [16,17]. Though various work-around measures have been taken to improve this problem, the maximum solubility of CS at physiological pH is still unsatisfactory. Licorice polysaccharide (LP) is a natural water soluble polysaccharide extracted from Chinese traditional medicine licorice that has been widely studied in recent years because of its excellent antimicrobial and immunoregulatory functions [18,19]. It is known that the aqueous solubility of CS is improved when formulated as a composite material with licorice polysaccharide. We hypothesize that by enhancing the solubility of CS, it will function better as a bacteriostatic material for wound dressings.

Many synthetic crosslinking agents used for CS-based hydrogel preparations are potentially cytotoxic [20–22]. This argues for the urgency to find a new hydrogel preparation method. Genipin, a natural cross-linker that is 10000 times less cytotoxic than glutaraldehyde, is finding a new role in replacing glutaraldehyde [23,24]. It is reported that CS hydrogels that are cross-linked with genipin are more resistant and resilient, less cytotoxic, and more impervious to *in vivo* degradation [25]. We are unaware of any reported studies that look into the bacteriostatic properties of genipin cross-linked CS/licorice polysaccharide composite hydrolgels. In this study, composite hydrogels were formulated with LP, CS, and genipin and characterized to evaluate their potential as a wound dressing.

2 Materials and Methods

2.1 Materials

Chitosan [deacetylation degree (DD) of 93%, Mw = ~210 KDa] was purchased from Shanghai Zhongqin Chemical Reagent Co., Ltd. (China). Genipin was purchased from Xi'an Kailai Biological Engineering Co., Ltd. (China). Licorice polysaccharide was purchased from West Anrui Bo Biological Technology Co., Ltd. (China). *Escherichia coli* and *Staphylococcus aureus* are from the Experimental

Center of Lanzhou University of Technology. Fibroblast cells NIH 3T3 were provided by the Bioresource Collection and Research Center, Shanghai (China). All other chemicals used in this work were of analytical grade and applied without further purification. Ultrapure water was prepared with a Milli-Q gradient A10 water purification system (Millipore Corporation, MA, US) and was directly used to prepare all solutions.

2.2 Preparation of Genipin Crosslinked Hydrogels

Chitosan (CS) was dissolved in 1% glacial acetic acid solution to afford a 3% CS-acetic acid solution. Fixed quantities of LP were added to distilled water and stirred at 40°C until dissolved at final concentrations of 2 wt% and 4 wt%. To form the hydrogels, genipin was added to distilled water and then stirred at room temperature until dissolved at final concentrations of 1 wt% and 1.5 wt%. Then, the LP, CS, and genipin solutions were mixed at a volume ratio of 1:1:1 and left to stand at room temperature until the hydrogels formed. The hydrogel sample compositions, designated by CSHa, CSLPHa-1, CSLPHa-2, CSLPHa-3, CSLPHa-4, CSLPHa-5, CSHb, CSLPHb-1, CSLPHb-2, CSLPHb-3, CSLPHb-4, and CSLPHb-5, are shown in Tab. 1.

Table 1: Compositions of various hydrogel formulations

	CSHa	CSLPHa-1	CSLPHa-2	CSLPHa-3	CSLPHa-4	CSLPHa-5	CSHb	CSLPHb-1	CSLPHb-2	CSLPHb-3	CSLPHb-4	CSLPHb-5
Chitosan (wt%)	3	3	3	3	3	3	3	3	3	3	3	3
LP (wt%)	0	2	4	6	8	10	0	2	4	6	8	10
Genipin (wt%)	1	1	1	1	1	1	1.5	1.5	1.5	1.5	1.5	1.5

2.3 Fourier Transform Infrared Spectroscopy (FTIR) Analysis of Hydrogels

FTIR spectroscopy (Fourier Transform Infrared Spectrometer, GER) in combination with Spectrum10™ software was used to analyze cross-sections of the gel samples. A spectral resolution of 4 cm^{-1} was achieved with four co-added scans over the spectral range between 4000 and 400 cm^{-1}. Each sample was placed in a sampling window while a force of 110–120 N and 75 N force was applied to different formulations of hydrogels. The spectra obtained were analyzed after baseline correction, normalization, and data-tune up processing [26].

2.4 Scanning Electron Microscope (SEM) Observations

The micromorphology of the hydrogels was observed with scanning electron microscopy (SEM; JSM-6010LV JEOL, Japan). The lyophilized rupture pieces of hydrogels were sprayed with gold and placed in a cabinet drier for 24 h before observation [27,28]. The pore sizes within the samples were quantified using Image J software. Five visual fields were selected randomly for each sample, and five pores were selected for measurement.

2.5 Swelling Ratio of Hydrogels

Hydrogels of the same weight were immersed in phosphate buffered saline (PBS, pH7.4) at room temperature. After 24 h, the hydrogels were carefully extracted from the bath, and water remaining on the surfaces of the samples was removed on filter paper. Then, the swollen hydrogel sample was weighed, and the swelling rate of the hydrogel was calculated according to the following formula:

$$\mathrm{SR} = (m_t - m_0)/m_0 \times 100\%$$

where SR is the swelling ratio of the hydrogel, m_t is the wet weight of the hydrogel after swelling, and m_0 is the initial weight of the hydrogel [29]. Measurements were performed in triplicate.

2.6 Rheological and Mechanical Properties of Hydrogels

The rheological properties of the samples were measured using a RS6000 rheometer (TA Instruments, GER). Solutions were prepared in advance and mixed just prior to testing, according to Tab. 1. One milliliter mixtures of the various samples were immediately loaded onto the lower stationary, thermostated rheometer plate (35 mm diameter), while the upper plate was adjusted to the predefined gap size (1 mm gap) at 25°C before formation of the hydrogel. After 5 min, the oscillatory measurement was carried out in a controlled deformation mode at a constant frequency of 1 Hz for the 7 min measurement [30].

2.7 In Vitro Degradation

CSLPH cylindrical samples were prepared and added to 5 mL PBS solution at different pH values (1.0, 7.4, 12.0) in three small beakers and incubated at 37°C. They were then extracted from the PBS medium at pre-determined time-points (7 d, 14 d, 21 d, 28 d), blotted with filter paper to remove buffer from the surfaces, and weighed immediately. The degradation rates of the samples were calculated by the following formula:

$$DR(\%) = (m_0 - m_t)/m_0 \times 100\%$$

Here, DR is the degradation rate of the hydrogel, m_0 is the fully swollen weight of the hydrogel before degradation, and m_t is the weight of the hydrogel after variable incubation periods [31]. Measurements were performed in triplicate.

2.8 Cytotoxicity Assay

Cell viability was assayed using the cell counting kit (CCK-8) from Wako Pure Chemical Industries (Osaka, Japan) according to the manufacturer's instructions [32,33]. Fibroblast NIH 3T3 cells were seeded in 96 well plates at 5×10^4 cells mL^{-1} and incubated overnight. The cells were then exposed to different conditions during this period, and the number of metabolically active cells was estimated after 24 h by measuring absorbance at 450 nm. Each condition was determined in triplicate.

2.9 Antibacterial Activity Evaluation

Bacteriostatic tests were carried out by the zone inhibition method [34]. The hydrogel samples were prepared under sterile conditions, then placed on petri dishes that had been coated with *E. coli* and *S. aureus* and incubated at 37°C for 24 h. The radius of the bacteriostatic areas surrounding each sample was measured with a ruler. The bacteriostatic tests were performed in triplicate for each sample.

2.10 Statistical Analysis

Statistical analyses were performed by Student's *T* tests. *p* values less than or equal to 0.05 imply a significant difference from the null hypothesis (Graph Pad Prism5). Results are shown as the value of the statistical mean and standard deviation of the mean.

3 Results and Discussion

3.1 The Formative Condition of Hydrogels

When the concentration of the genipin cross-linker was formulated at 1% or 1.5%, the resulting ratio of the LP was 2%, and 4%, and the hydrogels were found to be homogeneous. However, when the ratio of the LP was adjusted to be 6% or more, the hydrogels were found to divide into two layers. Consequently, only CSHa, CSLPHa-1, CSLPHa-2, CSHb, CSLPHb-1, and CSLPHb-2 were reserved for further experiments.

3.2 FTIR Analysis

FTIR spectroscopy of LP, CS, and CSLPHa-1 were measured in the range between 4000 and 400 cm^{-1} as shown in Fig. 1. The absorption band of CS between 3000 cm^{-1} and 3500 cm^{-1} is derived from the overlapping -OH stretch and -NH stretch vibrations. The bands at 2931 cm^{-1} and 1632 cm^{-1} are due to the absorption from the -CH stretch and amide group vibrations, respectively. The band at 1420 cm^{-1} is from the absorptions attributed to -CH_2 bending and-CH_3 group deformations. The band at 1383 cm^{-1} is produced by -CH_3 group symmetric stretching and -CH group bending. The band at 1047 cm^{-1} is attributed to asymmetric oxygen bridge stretching [35,36]. There is a weak absorption peak at 2974 cm^{-1}, which is due to the -CH stretching vibration [37]. The broad peak at 3440 cm^{-1} is caused by -OH group stretching, and the absorption peak at 1052 cm^{-1} may possibly result from-OH angular rocking. The latter two features indicate that LP contains an -OH group. The absorption peak at 1632 cm^{-1} is mainly caused by the -C=O asymmetric stretching vibration of the -CO group. The absorption peak at 1026 cm^{-1} results from the -CO stretching vibration that is caused by the -OH group angle vibration of -COOH, indicating that LP contains a -COOH group. The absorption peak at 835 cm^{-1} confirms that there is an α-pyran glycosidic bond in LP [38].
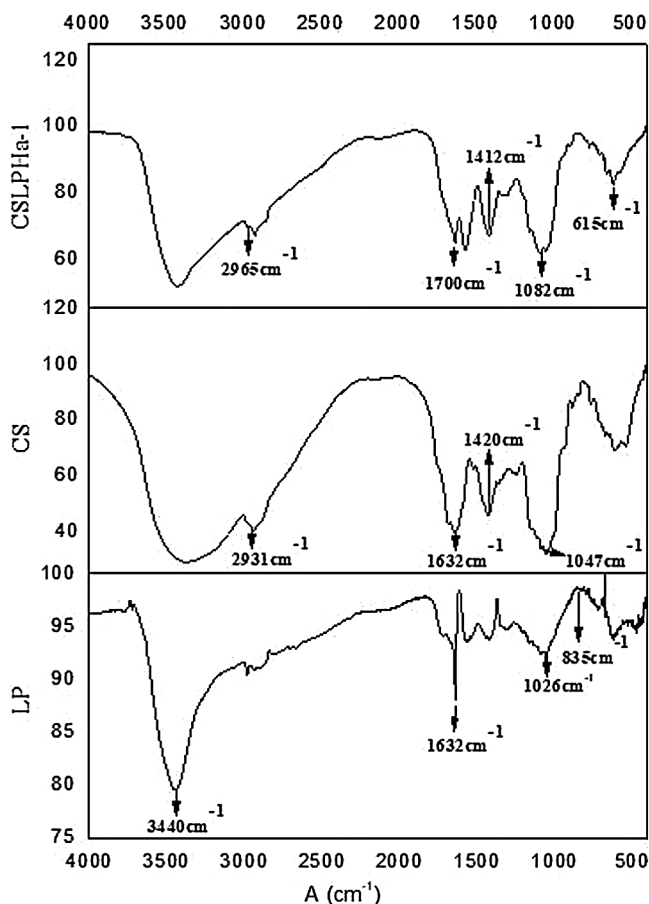

Figure 1: FTIR spectra of LP, CS, and CSLPHa-1

In the infrared spectrum of CSLPHa-1, the absorption band at 2965 cm^{-1} is assigned to the -CH stretch vibration, which shifts towards higher frequencies than what is found in CS and towards lower frequencies than that found in LP. This indicates that CS and LP interact with each other. The characteristic absorption

peak of the amide near 1700 cm^{-1} also disappears, which is probably due to the cross-linking reaction between CS and LP through genipin. The bands at 1568 cm^{-1}, 1412 cm^{-1}, and 1150 cm^{-1} are attributed to the -CH$_2$ curve and -CH$_3$ deformations. The bands at 1082 cm^{-1} and 615 cm^{-1} are attributed to the amine C-N group stretching modes and the -CH out of the plane bending modes, respectively [39].

3.3 Micromorphology of the Hydrogels

The micromorphology of the hydrogels is shown in Fig. 2. The hydrogels exhibit a three-dimensional mesh structure, which make it possible to absorb a large volume of wound exudate. Comparing CSLPHa-1 with CSHa, and CSLPHb-1 with CSHb, CSLPHa-1 and CSLPHb-1 possess a greater porous structure and thinner pore walls. In comparison, CSHb and CSLPHb-1, consisting of 2% LP and 3% CS, show a smaller pore size but more uniform size distribution (Tab. 2). In addition, some particles deposited in and between the pores of these gels result in thicker pore walls. CSLPHb-2 has thicker pore walls and many more deposits in and between the pores, which results from the concentration increase of LP from 2% to 4%. The patterns of change in CSHa, CSLPHa-1, and CSLPHa-2 follow the same trend. It appears that the increase of genipin in these formulations decreases the pore sizes of hydrogels and makes the structure more compact. Simultaneously, the increase in LP thickens the pore wall as it deposits in and between the pores.
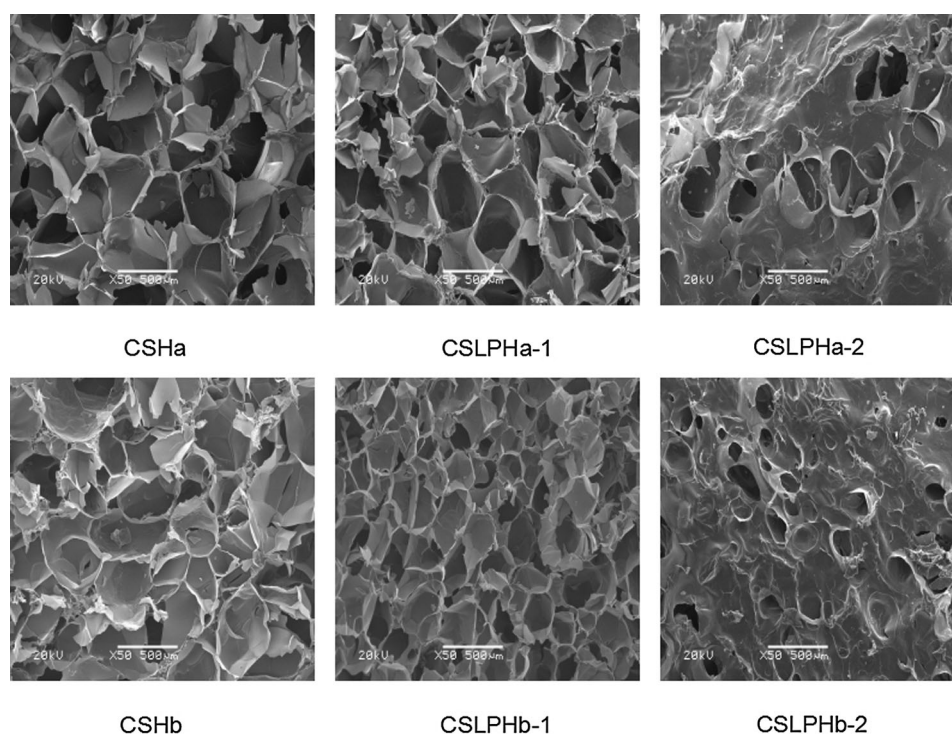

Figure 2: SEM micromorphology of the hydrogels

Table 2: Pore size of the hydrogels

Sample	CSHa	CSLPHa-1	CSLPHa-2	CSHb	CSLPHb-1	CSLPHb-2
Pore size (μm)	460 ± 30	280 ± 20	110 ± 20	400 ± 20	250 ± 30	90 ± 20

3.4 Swelling Ratio of Hydrogels

The swelling ratio of hydrogels is shown in Fig. 3. When the concentration of genipin is 1%, the swelling rates of CSHa, CSLPHa-1 and CSLPHa-2 become 1677%, 2126% and 1425%, respectively. When the concentration of genipin is 1.5%, the swelling ratios of CSHb, CSLPHb-1, and CSLPHb-2 become 1174%, 1512%, and 986%, respectively. The hydrogel is a hydrophilic polymer due to the presence of polarizable groups, such as -OH, $-NH_2$ and -COOH, that lead to a high degree of swelling [40]. In comparing the swelling ratios of CSLHa-1 and CSLPHb-1, we find that the swelling ratio of hydrogels decreases inversely as the concentration of genipin increases from 1% to 1.5%. Comparison of CSHa and CSHb, as well as CSLHa-2 and CSLPHb-2, show the same results. These are consistent with the micromorphology data. When the concentration of LP increases from 0% to 2%, the swelling ratio of both CSLPHa-1 and CSLPHb-1 increase. However, on raising the concentration of LP from 2% to 4%, the swelling ratio of CSLPHa-2 and CSLPHb-2 decreases. This can be explained by the microstructure of hydrogels. As shown in Fig. 2, when the concentration of LP is 2%, CSLPHa-1 and CSLPHb-1 possess more uniformity in pore size than CSHa and CSHb, which leads to a higher swelling ratio. In addition, the hydrophilic LP particles deposited in and between pores also improve the hydrophilicity of these compositions. With addition of greater concentrations of LP, there was too much polysaccharide deposited, the pore became too small to accommodate much water, and the swelling ratios decreased.
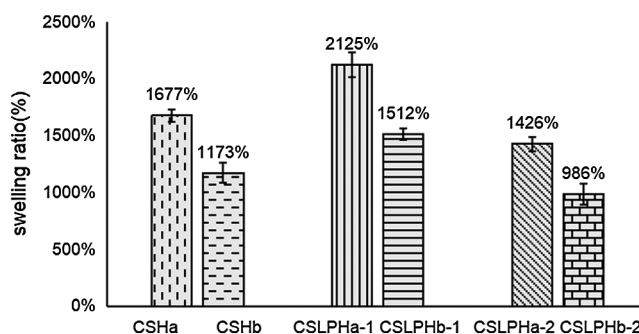

Figure 3: Swelling ratios of hydrogels in PBS solution at 37°C

3.5 Rheological Properties of Hydrogels

In rheology, the storage modulus (G') reflects the stiffness of hydrogels, while the loss modulus (G") relates to the material's ability to remove applied stresses through evolution of heat. Figs. 4a and 4b show the plots of G' and G" for the various formulations of CSHa and CSHb. At the end of the measurement cycle, the storage moduli (G') of CSHa and CSHb were found to be 1792 Pa and 1462 Pa, respectively. Similarly, the G' values of CSLPHa-1 and CSLPHb-1 were measured at 1205 Pa and 1005 Pa, while G'
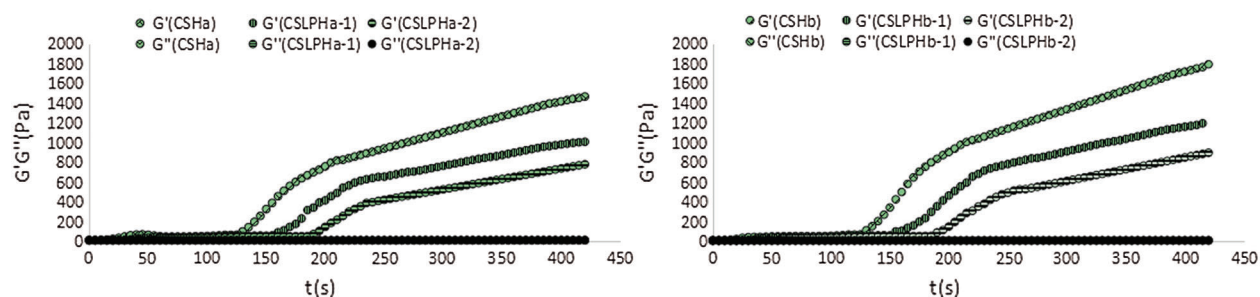

Figure 4: Storage modulus (G') and loss modulus (G") of CS-LP hydrogel formulations

of CSLPHa-2 and CSLPHb-2 were measured at 896 Pa and 777 Pa at corresponding times. We conclude, as expected, that a higher concentration of genipin produces higher stiffness of the hydrogels. Similarly, hydrogels made from 1.5% genipin retain higher shear moduli compared to hydrogels that contain 1% genipin in this series, though increasing concentrations of LP progressively decreases the overall value of the storage modulus. We consistently observe that in the range of 2–10 wt% LP, LP concomitantly reduces gel strength (G').

The condition found when G' >> G" indicates the formation of hydrogels [41–43]. About 130 s after the measurement commences, the storage modulus (G') of CSHa and CSHb becomes higher than the loss modulus (G") and increases gradually, which shows the formation of the hydrogels. However, the incremental rise in G'/G" arises about 40 s later in CSLPHa-1 and CSLPHb-1, and about 60 s later in CSLPHa-2 and CSLPHb-2. We suggest that LP delays the formation of the hydrogels by imposing water transport barriers.

3.6 In Vitro Degradation

An appropriate gel degradation rate would benefit the implementation of sustained and stable release of drugs that are encapsulated in the hydrogel wound dressing and ultimately reduce the cost of wound care. The in vitro degradation behavior of the hydrogels was tested in PBS at pH 7.4 [44,45]. As shown in Figs. 5A–5C the degradation rate at the end of 4 weeks of testing of the series of samples from CSHa to CSLPHb-2 were 70%, 58%, 49%, 57%, 49%, and 40%. Most of hydrogels lost 50% weight within 4 weeks, which demonstrates the applicability of the formulations as a wound dressing. The degradation rates of hydrogels comprising 1.5% genipin are a little slower than the rates of hydrogels made from 1% genipin. It is easy to understand how the greater content of crosslinker slows down the degradation rate. The degradation rate shows a dependency on the amount of added LP in a mass dependent manner. When the concentration of LP increased from 0% to 4 wt%, the degradation rate decreased from 70% to 49% in the 1% genipin group, and 56% to 40% in the 1.5% genipin group. The degradation rate of hydrogels at pH 12.0 is similar to that at pH 7.4 but is a little quicker at pH 1.0. This might be due to the fact that the amines formed by genipin and CS are easy to degrade under acidic conditions.

3.7 Cytotoxicity Assay

Though it has been confirmed by many researchers that genipin is a safer cross-linker than glutaraldehyde [46,47], the compatibility of the composite hydrogels needs to be verified. Human fibroblast NIH 3T3 cells were used as cell model to test the biocompatibility of the hydrogel formulations [48,49]. From Fig. 6 one can see that the cell viability of the 1% genipin group is 94%, 121%, 137% for CSHa, CSLPHa-1, and CSLPHa-2, respectively, which are all higher than the safety limit of 80%. We therefore believe that 1% genipin is a safe concentration of cross-linker for hydrogels. When the concentration of genipin increases to 1.5%, the cell viability drops to 74%. However, with the addition of LP, the cell viability increased to 85% in CSLPHb-1 gels and 115% in CSLPHb-2 gels. Thus, the LP either promotes the cell proliferation properties or inhibits the cytotoxicity of genipin. On increasing the polysaccharide content, the effect becomes more conspicuous. This result suggests CS hydrogels have significantly improved prospects for use in many applications as a wound dressing.

3.8 Antibacterial Activity Evaluation

The radii of the bacteriostatic areas of different hydrogel formulations are shown in Tab. 3, and the inhibition rates of the corresponding hydrogels are shown in Fig. 7. The series of formulations produced a range of inhibition rates between 51% and 81% for *Escherichia coli*, and a range between 49% and 75% for *Staphylococcus aureus*. There was no significant difference between formulations in the groups
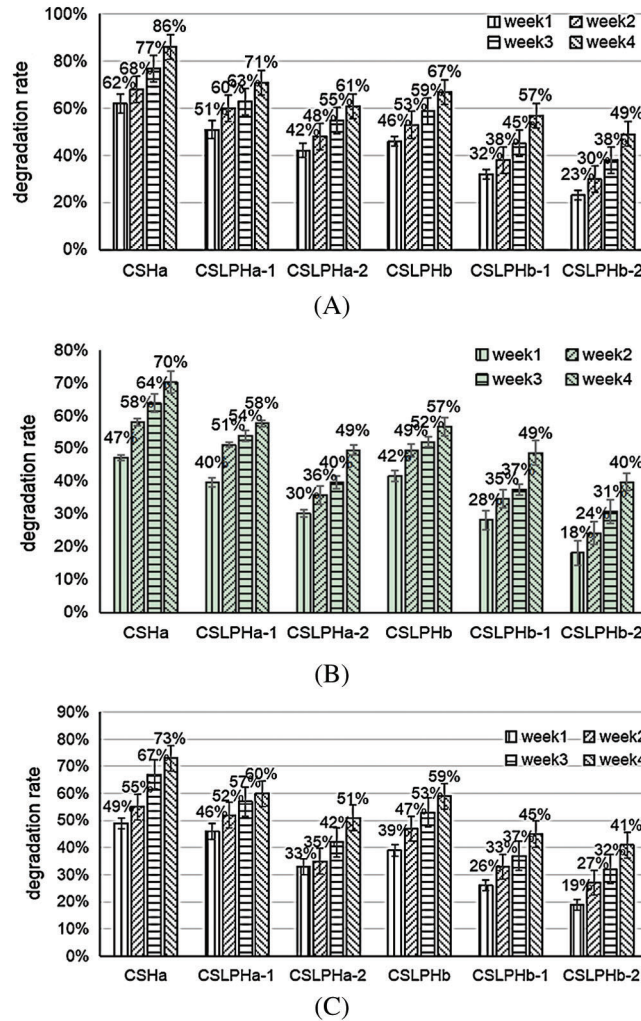
Figure 5: *In vitro* degradation profile of hydrogels in PBS solution with pH 1.0 (A), pH 7.4 (B) and pH 12.0 (C) at 37°C
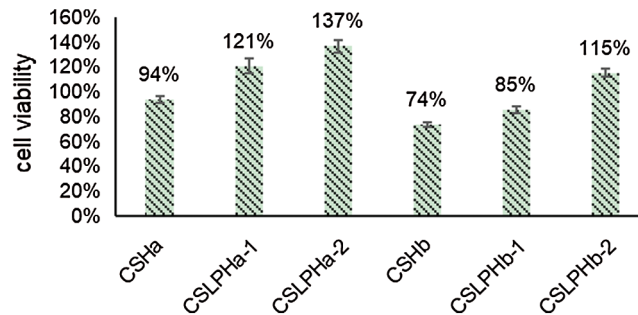

Figure 6: *In vitro* cytotoxicity of hydrogels against 3T3 cells was confirmed by CCK-8 assay

Table 3: Radius of the bacteriostatic area of hydrogels

		Radius of the bacteriostatic area(cm)						
	Positive control	CSHa	CSLPHa-1	CSLPHa-2	CSHb	CSLPHb-1	CSLPHb-2	
E. coli	1	3.10	1.56	1.78	2.40	1.64	1.96	2.41
	2	3.66	2.00	2.55	2.68	2.12	2.62	3.07
	3	3.45	1.73	2.22	2.90	1.92	2.33	2.78
S. aureus	1	3.20	1.41	1.82	2.20	1.64	1.80	2.24
	2	2.80	1.42	1.79	2.07	1.34	1.81	2.16
	3	3.32	1.71	2.23	2.59	1.77	2.04	2.60
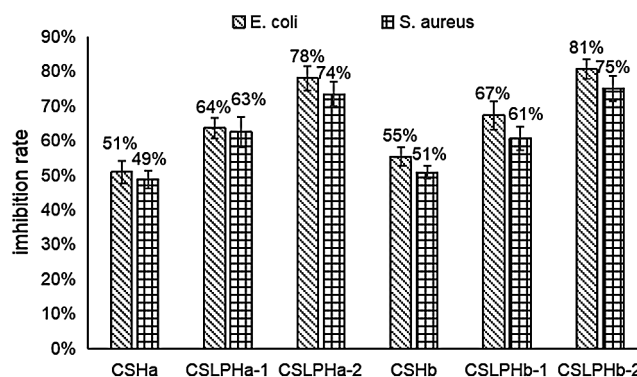
Figure 7: Inhibition rates against *E. coli* and *S. aureus* colony growth for different hydrogels

containing the 1% genipin and 1.5% genipin, indicating that the crosslinker genipin does not contribute to the bacteriostasis. The bacteriostatic inhibition does improve significantly after the addition of LP, and the inhibition rates against *Escherichia coli* and *Staphylococcus aureus* both increase with increased content of the polysaccharide. Since inhibition occurs for both gram-positive and gram-negative bacteria, this makes these hydrogels suitable for wound dressing.

4 Conclusions

We conclude that the porous structures and moderate stiffness make hydrogels suitable for wound dressings. Though LP added in the hydrogels reduces the mechanical strength and delays the gelation and degradation time of the hydrogels, it substantially improves the cyto-compatibility of the restorative environment to invading repair tissues and increases bacteriostatic inhibition. CSLPH-2, comprised of 1% genipin, 3% CS, and 4% LP, showed the best antibacterial and cell proliferation promoting activity. CSLPH-2 possesses a moderate swelling capacity and moderately slow degradation rate, making it a suitable formulation for covering chronic infection wounds. These results reveal new alternatives to clinicians and researchers who want to improve antibacterial properties and cyto-compatibility of CS hydrogels. However, the mechanism by which LP acts as a bacteriostat and promotes fibroblast proliferation is still unclear. We hope to identify the critical features of its structure and explore its interaction with CS in hydrogels in further research.

5 Author Contributions

Haiwei Ren and Hui Bao equally contributed to this work and should be considered co-first author.

Conflicts of Interest: The authors declare that they have no conflicts of interest to report regarding the present study.

References

1. Rasuli, S., Lotfi, M., Seyedamini, B., Zamanzadeh, V., Naghili, B. (2013). The effects of biological, synthetic and traditional dressing on pain intensity of burn wound in children. *Iran Journal of Nursing, 26(85),* 15–25.

2. Koehler, J., Brandl, F. P., Goepferich, A. M. (2018). Hydrogel wound dressings for bioactive treatment of acute and chronic wounds. *European Polymer Journal, 100,* 1–11. DOI 10.1016/j.eurpolymj.2017.12.046.

3. Balakrishnan, B., Mohanty, M., Umashankar, P. A. (2005). Evaluation of an in situ forming hydrogel wound dressing based on oxidized alginate and gelatin. *Biomaterials, 26(32),* 6335–6342. DOI 10.1016/j.biomaterials.2005.04.012.

4. Murakami, K., Aoki, H., Nakamura, S., Nakamura, S., Megumi Takikawa, M. et al. (2010). Hydrogel blends of chitin/chitosan, fucoidan and alginate as healing-impaired wound dressings. *Biomaterials, 31(1),* 83–90. DOI 10.1016/j.biomaterials.2009.09.031.

5. Lin, K. S., Wang, S. Y., Fan, L. J., Pan, D. Y., Xian, C. J. et al. (2017). Adipose-derived stem cells seeded in pluronic f-127 hydrogel promotes diabetic wound healing. *Journal of Surgical Research, 217,* 63–74. DOI 10.1016/j.jss.2017.04.032.

6. Qu, J., Zhao, X., Liang, Y., Zhang, T., Ma, P. X. et al. (2018). Antibacterial adhesive injectable hydrogels with rapid self-healing, extensibility and compressibility as wound dressing for joints skin wound healing. *Biomaterials, 183,* 185–199. DOI 10.1016/j.biomaterials.2018.08.044.

7. Li, M., Chen, J., Shi, M., Zhang, H. L., Ma, P. X. et al. (2019). Electroactive anti-oxidant polyurethane elastomers with shape memory property as non-adherent wound dressing to enhance wound healing. *Chemical Engineering Journal, 375,* 121999. DOI 10.1016/j.cej.2019.121999.

8. Liang, Y., Zhao, X., Hu, T., Chen, B., Yin, Z. et al. (2019). Adhesive hemostatic conducting injectable composite hydrogels with sustained drug release and photothermal antibacterial activity to promote full-thickness skin regeneration during wound healing. *Small, 15(12),* e1900046. DOI 10.1002/smll.201900046.

9. Matica, M. A., Aachmann, F. L., Tøndervik, A., Sletta, H., Ostafe, V. (2019). Chitosan as a wound dressing starting material: antimicrobial properties and mode of action. *International Journal of Molecular Sciences, 20(23),* 5889. DOI 10.3390/ijms20235889.

10. Yang, W., Owczarek, J. S., Fortunati, E., Kozanecki, M., Mazzaglia, A. et al. (2016). Antioxidant and antibacterial lignin nanoparticles in polyvinyl alcohol/chitosan films for active packaging. *Industrial Crops and Products, 94,* 800–811. DOI 10.1016/j.indcrop.2016.09.061.

11. Yang, W., Owczarek, J. S., Fortunati, E., Kozanecki, M., Mazzaglia, A. et al. (2018). Polyvinyl alcohol/chitosan hydrogels with enhanced antioxidant and antibacterial properties induced by lignin nanoparticles. *Carbohydrate Polymers, 181,* 275–284. DOI 10.1016/j.carbpol.2017.10.084.

12. Zhao, X., Wu, H., Guo, B., Dong, R., Qiu, Y. et al. (2017). Antibacterial anti-oxidant electroactive injectable hydrogel as self-healing wound dressing with hemostasis and adhesiveness for cutaneous wound healing. *Biomaterials, 122,* 34–47. DOI 10.1016/j.biomaterials.2017.01.011.

13. Zhao, X., Guo, B. L., Wu, H., Liang, Y. P., Ma, P. X. (2018). Injectable antibacterial conductive nanocomposite cryogels with rapid shape recovery for noncompressible hemorrhage and wound healing. *Nature Communications, 9(1),* 2784. DOI 10.1038/s41467-018-04998-9.

14. Liang, Y. P., Zhao, X., Hu, T. L., Han, Y., Guo, B. L. (2019). Mussel-inspired, antibacterial, conductive, antioxidant, injectable composite hydrogel wound dressing to promote the regeneration of infected skin. *Journal of Colloid and Interface Science, 556,* 514–528. DOI 10.1016/j.jcis.2019.08.083.

15. He, J. H., Shi, M. T., Liang, Y. P., Guo, B. L. (2020). Conductive adhesive self-healing nanocomposite hydrogel wound dressing for photothermal therapy of infected full-thickness skin wounds. *Chemical Engineering Journal, 384,* 124888. DOI 10.1016/j.cej.2020.124888.

16. Coviello, T., Matricardi, P., Marianecci, C., Alhaique, F. (2007). Polysaccharide hydrogels for modified release formulations. *Journal of Controlled Release, 119(1),* 5–24. DOI 10.1016/j.jconrel.2007.01.004.

17. Rinaudo, M. (2007). Chitin and chitosan: properties and applications. *Cheminform, 31(7),* 603–632. DOI 10.1016/j.progpolymsci.2006.06.001.

18. Bigi, A., Cojazzi, G., Panzavolta, S., Roveri, N., Rubini, K. (2002). Stabilization of gelatin films by crosslinking with genipin. *Biomaterials, 23(24),* 4827–4832. DOI 10.1016/S0142-9612(02)00235-1.

19. Tian, Y. H., Yang, Z. Y., Liu, L. F., Liu, N. L., Guo, Y. (2017). Extraction, purification and biological activity of polysaccharide from glycyrrhiza uralcnsis in gansu. *Science & Technology of Food Industry, 38(10),* 296–302. DOI 10.13386/j.issn1002-0306.2017.10.048.

20. Di, M. A., Sittinger, M., Risbud, M. V. (2005). Chitosan: a versatile biopolymer for orthopaedic tissue-engineering. *Biomaterials, 26(30),* 5983–5990. DOI 10.1016/j.biomaterials.2005.03.016.

21. Monteiro, O. A. C., Airoldi, C. (1999). Some studies of crosslinking chitosan-glutaraldehyde interaction in a homogeneous system. *International Journal of Biological Macromolecules, 26(2–3),* 119–128. DOI 10.1016/S0141-8130(99)00068-9.

22. Sung, H. W., Huang, R. N., Huang, L. L. H., Tsai, C. C. (1999). *In vitro* evaluation of cytotoxicity of a naturally occurring cross-linking reagent for biological tissue fixation. *Journal of Biomaterials Science, Polymer Edition, 10 (1),* 63–78. DOI 10.1163/156856299X00289.

23. Gough, J. E., Scotchford, C. A., Downes, S. (2002). Cytotoxicity of glutaraldehyde crosslinked collagen/poly (vinyl alcohol) films is by the mechanism of apoptosis. *Journal of Biomedical Materials Research, 61(1),* 121–130. DOI 10.1002/jbm.10145.

24. Muzzarelli, R. A. A. (2009). Genipin-crosslinked chitosan hydrogels as biomedical and pharmaceutical aids. *Carbohydrate Polymers, 77(1),* 1–9. DOI 10.1016/j.carbpol.2009.01.016.

25. Bellé, A. S., Hackenhaar, C. R., Spolidoro, L. S., Rodrigues, E., Klein, M. P. et al. (2018). Efficient enzyme-assisted extraction of genipin from genipap (*Genipa americana* L.) and its application as a crosslinker for chitosan gels. *Food Chemistry, 246(4),* 266–274. DOI 10.1016/j.foodchem.2017.11.028.

26. Li, S. M., Fu, L. H., Ma, M. G., Zhu, J., Sun, R. C. et al. (2012). Simultaneous microwave-assisted synthesis, characterization, thermal stability, and antimicrobial activity of cellulose/AgCl nanocomposites. *Biomass and Bioenergy, 47(4),* 516–521. DOI 10.1016/j.biombioe.2012.10.012.

27. Luo, P., Nie, M., Wen, H., Xu, W., Fan, L. et al. (2018). Preparation and characterization of carboxymethyl chitosan sulfate/oxidized konjac glucomannan hydrogels. *International Journal of Biological Macromolecules, 113,* 1024–1031. DOI 10.1016/j.ijbiomac.2018.01.101.

28. Lewis, P. L., Green, R. M., Shah, R. N. (2018). 3D-printed gelatin scaffolds of differing pore geometry modulate hepatocyte function and gene expression. *Acta Biomaterialia, 69,* 63–70. DOI 10.1016/j.actbio.2017.12.042.

29. Kundu, B., Kundu, S. C. (2012). Silk sericin/polyacrylamide in situ forming hydrogels for dermal reconstruction. *Biomaterials, 33(30),* 7456–7467. DOI 10.1016/j.biomaterials.2012.06.091.

30. Zhang, Y. S., Jiang, R. L., Fang, A., Zhang, Y. Y., Wu, T. F. et al. (2019). A highly transparent, elastic, injectable sericin hydrogel induced by ultrasound. *Polymer Testing, 77,* 105890. DOI 10.1016/j.polymertesting.2019.05.006.

31. Wang, Z., Zhang, Y. S., Zhang, J. X., Huang, L., Liu, J. et al. (2014). Exploring natural silk protein sericin for regenerative medicine: an injectable, photoluminescent, cell-adhesive 3D hydrogel. *Scientific Reports, 4(1),* 7064. DOI 10.1038/srep07064.

32. Zhang, B., Gao, L., Gu, L., Yang, H., Luo, Y. et al. (2017). High-resolution 3D bioprinting system for fabricating cell-laden hydrogel scaffolds with high cellular activities. *Procedia Cirp, 65,* 219–224. DOI 10.1016/j.procir.2017.04.017.

33. Fan, Z., Liu, B., Wang, J., Zhang, S., Lin, Q. et al. (2014). A novel wound dressing based on Ag/graphene polymer hydrogel: effectively kill bacteria and accelerate wound healing. *Advanced Functional Materials, 24(25),* 3933–3943. DOI 10.1002/adfm.201304202.

34. Basini, G., Spatafora, C., Tringali, C., Bussolati, S., Grasselli, F. (2014). Effects of a ferulate-derived dihydrobenzofuran neolignan on angiogenesis, steroidogenesis, and redox status in a swine cell model. *Journal of Biomolecular Screening, 19(9),* 1282–1289. DOI 10.1177/1087057114536226.

35. Wilkins, W. H., Harris, G. C. M. (2010). Investigation into the production of bacteriostatic substances by fungi. *Annals of Applied Biology, 30(3),* 226–229. DOI 10.1111/j.1744-7348.1943.tb06193.x.

36. Brugnerotto, J., Lizardi, J., Goycoolea, F. M., Arguellesmonal, W., Desbrieres, J. et al. (2001). An infrared investigation in relation with chitin and chitosan characterization. *Polymer, 42(8),* 3569–3580. DOI 10.1016/S0032-3861(00)00713-8.

37. Zhang, W. J. (1999). *Biochemical research technology of sugar complex*. China: Zhejiang University Press.

38. Wang, Q., Lee, F., Wang, X. (2004). Isolation and purification of inflacoumarin and licochalcone a from licorice by high-speed counter-current chromatography. *Journal of Chromatography A, 1048(1),* 51–57. DOI 10.1016/S0021-9673(04)01086-6.

39. Ouyang, Q. Q., Hu, Z., Lin, Z. P., Quan, W. Y., Deng, Y. F. et al. (2018). Chitosan hydrogel in combination with marine peptides from tilapia for burns healing. *International Journal of Biological Macromolecules, 112,* 1191–1198. DOI 10.1016/j.ijbiomac.2018.01.217.

40. Afshari, M. J., Sheikh, N., Afarideh, H. (2015). PVA/CM-chitosan/honey hydrogels prepared by using the combined technique of irradiation followed by freeze-thawing. *Radiation Physics and Chemistry, 113,* 28–35. DOI 10.1016/j.radphyschem.2015.04.023.

41. Lin, Y. W., Xu, C., Lu, C. H. (2000). Preparation of carboxymethyl chitosan by ultrasonic radiation. *Ion Exchange & Adsorption, 16(1),* 54–59. DOI 10.16026/J.CNKI.IEA.2000.01.008.

42. Zhang, H. B. (2014). *Polysaccharides and their modified materials*, pp. 3–36. Beijing: Chemical Industry Press.

43. Afzal, S., Maswal, M., Dar, A. A. (2018). Rheological behavior of pH responsive composite hydrogels of chitosan and alginate: characterization and its use in encapsulation of citral. *Colloids & Surfaces B: Biointerfaces, 169,* 99–106. DOI 10.1016/j.colsurfb.2018.05.002.

44. Zhang, W., Ren, G., Xu, H., Zhang, J., Liu, H. et al. (2016). Genipin cross-linked chitosan hydrogel for the controlled release of tetracycline with controlled release property, lower cytotoxicity, and long-term bioactivity. *Journal of Polymer Research, 23(8),* 126. DOI 10.1007/s10965-016-1059-5.

45. Chronopoulou, L., Toumia, Y., Cerroni, B., Pandolfi, D., Paradossi, G. et al. (2016). Biofabrication of genipin-crosslinked peptide hydrogels and their use in the controlled delivery of naproxen. *New Biotechnology, 37,* 138–143. DOI 10.1016/j.nbt.2016.04.006.

46. Patel, S., Srivastava, S., Singh, M. R., Singh, D. (2018). Preparation and optimization of chitosan-gelatin films for sustained delivery of lupeol for wound healing. *International Journal of Biological Macromolecules, 107,* 1888–1897. DOI 10.1016/j.ijbiomac.2017.10.056.

47. Zhao, J., Yan, Y., Shang, Y., Du, Y., Long, L. et al. (2016). Thermosensitive elastin-derived polypeptide hydrogels crosslinked by genipin. *International Journal of Polymeric Materials and Polymeric Biomaterials, 66(8),* 369–377. DOI 10.1080/00914037.2016.1217534.

48. Hsu, C. L., Lin, Y. J., Ho, C. T., Yen, G. C. (2012). Inhibitory effects of garcinol and pterostilbene on cell proliferation and adipogenesis in 3T3-l1 cells. *Food & Function, 3(1),* 49–57. DOI 10.1039/C1FO10209E.

49. Nuttelman, C. R., Mortisen, D. J., Henry, S. M., Anseth, K. S. (2001). Attachment of fibronectin to poly (vinyl alcohol) hydrogels promotes NIH3T3 cell adhesion, proliferation, and migration. *Journal of Biomedical Materials Research, 57(2),* 217–223.